Liquid-Crystalline Polyimides. 11. Thermotropic Aromatic Poly(Ester-Imide)S Based on Biphenyl-3,3',4,4' -Tetracarboxylic Imide

Hans R. Kricheldorf[a]; Volker Linzer[a]; Christof Bruhn[a]

[a] Institut für Technische und Makromolekulare Chemie Universität, Hamburg, Germany

PLEASE SCROLL DOWN FOR ARTICLE

LIQUID-CRYSTALLINE POLYIMIDES. 11. THERMOTROPIC AROMATIC POLY(ESTER-IMIDE)S BASED ON BIPHENYL-3,3′,4,4′-TETRACARBOXYLIC IMIDE

HANS R. KRICHELDORF,* VOLKER LINZER, and CHRISTOF BRUHN

Institut für Technische und Makromolekulare Chemie
Universität Hamburg
Bundesstrasse 45, D-20146 Hamburg, Germany
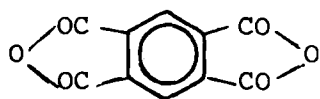
ABSTRACT

    Four acetylated diphenols were prepared from pyromellitic anhydride (PMDA) or biphenyl-3,3′,4,4′-tetracarboxylic anhydride (BTCA) and 3-aminophenol or 4-aminophenol. The melting points of three of these acetylated diphenols were below 400°C and allowed polycondensations with various aromatic dicarboxylic acids in the form of their bistrimethylsilylesters. All poly(ester-imide)s derived from 3-aminophenol formed isotropic melts. In contrast, all poly(ester-imide)s derived from 4-aminophenol and BTCA form a nematic melt. The poly(ester-imide)s were characterized by elemental analyses, inherent viscosities, DSC measurements, WAXS powder patterns, and optical microscopy.

INTRODUCTION

    Fully aromatic, thermotropic poly(ester imide)s were first described in patents of DuPont [1] and Idemitsu Petrochemical [2]. In both cases, copolyesters of three or more components were reported with only one monomer being an imide, namely *N*-(4′-carboxyphenyl)trimellitimide. Because all other comonomers possess the capability of forming liquid-cyrstalline (LC) polyesters, these copolyesters do not give any information on the mesogeneity of this imide monomer.
    The present work is part of a broader study of structure–property relationships of aromatic poly(ester-imide)s [3–6]. An important aim of these studies is to eluci-

date which type of imide structure meets the requirements of a mesogenic unit. In the present work, aromatic polyesters of diphenols derived from pyromellitic anhydride (PMDA) **1** or biphenyl-3,3',4,4'-tetracarboxylic anhydride (BTCA) **2** were synthesized and characterized.
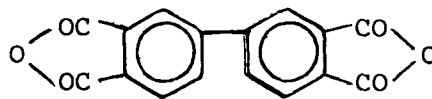
EXPERIMENTAL

Materials

Pyromellitic anhydride (PMDA) and biphenyl-3,3',4,4'-tetracarboxylic anhydride (BTCA) were gifts of Bayer AG (Krefeld, Germany). They were purified by recrystallization from mixtures of toluene and acetic anhydride. 3- and 4-Aminophenol were also gifts of Bayer AG. They were used without further purification. Dimethylformamide (DMF) was distilled over P_4O_{10} in vacuo.

Syntheses of Imid Monomers (see Table 1)

PMDA or BTCA (0.1 mol) and an aminophenol (0.2 mol) were heated in dry DMF (500 ml) at 80°C for 4 hours. Then acetic anhydride (0.5 mol) and pyridine

TABLE 1. Yields and Properties of Acetylated Diphenols Prepared from Aminophenols and PMDA or BTCA

Formula	Yields, %	mp,[a] °C	Elementary formula (formula weight)		Elemental analyses		
					C	H	N
3a	31	>500	$C_{26}H_{16}N_2O_6$	Calcd.	64.47	3.33	5.78
			(484.42)	Found	63.93	3.02	5.64
3b	56	314–344	$C_{26}H_{16}N_2O_6$	Calcd.	64.47	3.33	5.78
			(484.42)	Found	64.58	3.25	3.85
4a	55	295–297	$C_{32}H_{20}N_2O_6$	Calcd.	68.57	3.60	5.00
			(560.52)	Found	68.63	3.46	5.07
4b	56	342[b]	$C_{32}H_{20}N_2O_6$	Calcd.	68.57	3.60	5.00
			(560.52)	Found	68.68	3.46	5.01

[a]Determined by differential calorimetry at a heating rate of 20°C/min.
[b]See Fig. 1.

(10 mL) were added, and the reaction mixture was stirred at 120°C for 12 hours. After cooling, the reaction mixture was poured into cold water (2.5 L). The crystallized product was filtered off, washed with water, and recrystallized from mixtures of dioxane and a little water.

Silylation of Dicarboxylic Acids (see Table 2)

A dicarboxylic acid (0.4 mol) and hexamethyldisilazane (p.5 mol) were refluxed in dry toluene until the evolution of NH_3 had ceased. The reaction was then concentrated in vacuo, and the product was distilled over a short-path apparatus at a 160–230°C bath temperature in a vacuum of 10^{-3} bar.

Polycondensations

An acetylated diphenol (10 mmol), a silylated dicarboxylic acid (10 mmol), and titanium tetraisopropoxide (0.01 mol dissolved in toluene) were weighed into a cylindrical glass reactor equipped with a stirrer and gas-inlet and -outlet tubes. The reaction vessel was placed into a metal bath preheated to 150–180°C, and the temperature was rapidly raised to 300–330°C to obtain a homogeneous melt. Then the temperature was lowered to 260–280°C so that a smooth condensation took place. The temperature was then raised in 20°C steps up to 320°C over a period of 4 hours. Finally, the reaction mixture (which in most cases solidified) was heated at 320–325°C of 0.5 hour without vacuum and for 0.5 hour with vacuum. After cooling, the crude reaction product was ground and extracted with hot acetone or dissolved in a mixture of CH_2Cl_2 and trifluoroacetic (volume ratio 4:1) and precipitated into methanol.

TABLE 2. Yields and Properties of Silylated Aromatic Dicarboxylic Acids

Formula	Yields, %	mp,[a] °C	Elementary formula (formula weight)		Elemental analyses		
					C	H	S
5	92		$C_{20}H_{26}O_5Si_2$	Calcd.	59.67	6.51	—
			(402.60)	Found	59.52	6.51	—
6a	87	110–112	$C_{20}H_{26}O_4SSi_2$	Calcd.	57.38	6.26	7.66
			(418.66)	Found	57.22	6.19	8.02
6b	89	119–120	$C_{20}H_{25}CO_4SSi_2$	Calcd.	53.02	5.56	7.08
			(454.11)	Found	53.49	5.57	7.31
7	92	108–110	$C_{26}H_{30}O_5Si_2$	Calcd.	65.24	6.32	—
			(478.78)	Found	65.19	6.35	—
8	95	116–118	$C_{18}H_{24}O_4Si_2$	Calcd.	59.96	6.71	
			(360.56)	Found	60.13	6.75	

Measurements

The inherent viscosities were measured with an automated Ubbelohde viscometer thermostated at 20°C.

The DSC measurements were conducted with a Perkin-Elmer DSC-4 in aluminum pans under nitrogen at a heating and cooling rate of 20°C/min.

The WAXS powder patterns were recorded with a Siemens D-500 diffractometer by means of CuK$_\alpha$ radiation. WAXS and SAXS measurements were also conducted with synchrotron radiation ($\lambda = 1.50$ Å) at Hasylab (DESY), Hamburg, Germany. A heating and cooling rate of 20°C/min, a vacuum oven, and a one-dimensional position-sensitive detector were used for all these measurements.
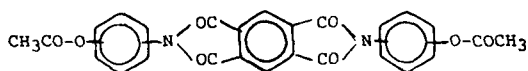
RESULTS AND DISCUSSION

Syntheses

Starting from the commercial anhydrides **1** and **2**, the acetylated diphenols **3a**, **3b** and **4a**, **4b** were prepared. The syntheses of these monomers were conducted by a standard "one-pot procedure" using acetic anhydride as the dehydrating reagent (Table 1). The melting points of all monomers were determined by differential scanning calorimetry. It was found that **3a** melts and decomposes above 500°C; consequently, this compound is not useful as a monomer for thermal polycondensations. The melting points of the other three monomers are below 400°C and allow, in principle, polycondensations with various aromatic dicarboxylic acids. The DSC measurements of **4b** revealed that this monomer undergoes several interesting phase transitions which will be discussed below.
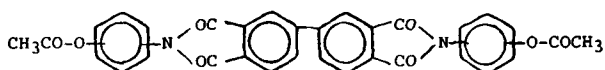
When preliminary polycondensations of **3b** and **4b** were conducted with phenylthioterephthalic acid or naphthalene-2,6-dicarboxylic acid, initial reaction temperatures above 310°C were required to obtain a homogeneous melt. However, at such high temperatures the dicarboxylic acid began to decompose by decarboxylation and cyclization [7], and only black oils or tars were obtained. Other polycondensation methods based on free diphenols or silylated diphenols were not helpful because hydrolysis of the acetate groups of **3a**, **3b** and **4a**, **4b** is more or less accompanied by partial hydrolysis of the imide rings.

Due to the failure of the standard polycondensation methods, a new approach was used which consists of the condensation of monomers **3b** and **4a**, **4b** with the silylated dicarboxylic acids **5–8**. This recently reported new polycondensation method [8, 9] combines several advantages for the purpose of this work. First, the melting points of the silylated dicarboxylic acids are much lower than those of the free acids (Table 2), and mixtures with monomers **3b** and **4a**, **4b** form homogeneous melts below 330°C or even below 300°C. Second, the silylation stabilizes the carboxyl groups against decarboxylation. Third, acidic protons which catalyze side reactions, such as the Fries rearrangement, are absent (Eq. 1). The new monomers **5–8** are easily prepared by silylation of the corresponding dicarboxylic acids with hexamethyldisilazane (or chlorotrimethylsilane + triethylamine) in refluxing tolu-
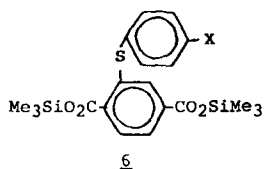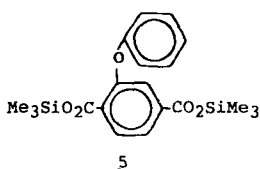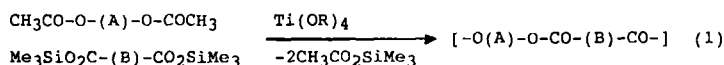
ene or dioxane (Table 2). Monomers **5**, **6a**, **6b**, and **8** were purified by distillation, whereas monomer **7** was used as the crude product.
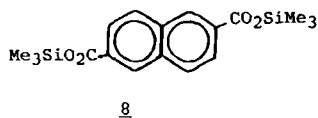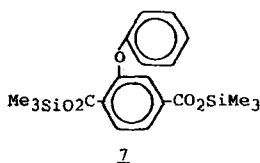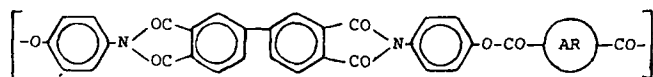
$$CH_3CO-O-(A)-O-COCH_3 \qquad Ti(OR)_4$$
$$Me_3SiO_2C-(B)-CO_2SiMe_3 \qquad \xrightarrow{\quad\quad} \quad [-O(A)-O-CO-(B)-CO-] \quad (1)$$
$$-2CH_3CO_2SiMe_3$$

a: X = H,   **b:** X = Cl

The polycondensation of acetylated diphenols with silylated dicarboxylic acids is catalyzed by titanium tetraisopropoxide [8], and thus this catalyst was added to all polycondensations of this work. The polycondensations were started at temperatures around 270–280°C and completed at 320–325°C. In this way the poly(ester-imide)s **9a**, **9b**, **10a–d**, and **11a–e** were prepared. Their yields and properties are summarized in Tables 3 and 4.

$\underline{9}$

$\underline{a}$: (AR) = $\underline{b}$: (AR) =

$\underline{10}$

$\underline{a}$: (AR) = $\underline{b}$: (AR) =

$\underline{c}$: (AR) = $\underline{d}$: (AR) =

$\underline{11a}$ - $\underline{e}$

$\underline{a}$: (AR) = $\underline{b}$: (AR) =

$\underline{c}$: (AR) = $\underline{d}$: (AR) =

$\underline{e}$: (AR) =
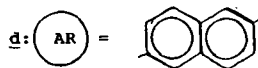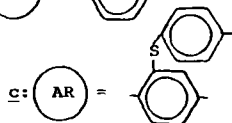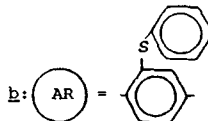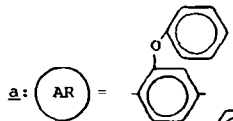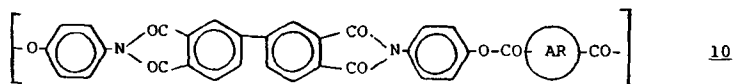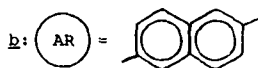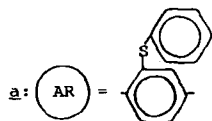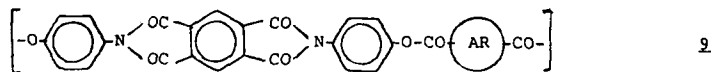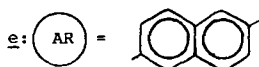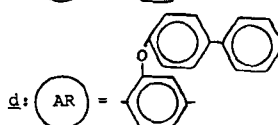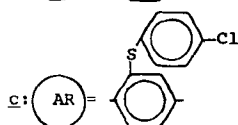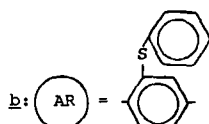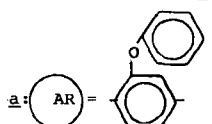
Properties of Monomer 4b

The DSC measurements of monomer **4b** conducted with a heating and cooling rate of 20°C/min revealed three endotherms in the heating curve and three exotherms in the cooling trace (Fig. 1). WAXS measurements conducted with synchrotron radiation, again at a heating and cooling rate of 20°C/min, indicate that all wide-angle reflections disappear between 340 and 345°C (Fig. 2). This result proves that the endotherm at 342°C represents the melting point. The SAXS measurements (Fig. 3) show that a small-angle reflection at 0.99° (89 Å) disappears in the same temperature range, whereas a reflection at 3.16° (28Å) gains in intensity. The distance of 28 Å agrees with the length of the molecule and indicates the formation of a smectic phase. The absence of wide-angle reflections suggests a smectic-A phase.

TABLE 3. Yields and Properties of Poly(Ester-imide)s **9a**, **9b**, and **10a–c** Based on 3-Aminophenol, PMDA, or BTCA

Polymer formula	Yields, %	η_{inh},[a] dL/g	T_g,[b] °C	T_m,[c] °C	Elementary formula (formula weight)		Elemental analyses			
							C	H	N	S
9a	94	Insoluble	238	401	$C_{36}H_{18}N_2O_8S$ (638.61)	Calcd.	67.71	2.84	4.39	5.02
						Found	66.38	3.06	4.22	4.63
9b	93	Insoluble	—	—	$C_{34}H_{16}N_2O_8$ (580.51)	Calcd.	70.35	2.78	4.83	—
						Found	68.71	2.91	4.55	—
10a	96	0.30	197	—	$C_{42}H_{22}N_2O_9$ (698.64)	Calcd.	72.21	3.17	4.01	—
						Found	71.30	3.23	3.94	—
10b	97	0.27	199	—	$C_{42}H_{22}N_2O_9S$ (714.71)	Calcd.	70.58	3.10	3.92	4.49
						Found	70.22	3.30	4.01	4.27
10c	96	0.30	195	—	$C_{42}H_{21}N_2O_8SCl$ (749.15)	Calcd.	67.34	2.83	3.74	4.28
						Found	67.18	3.04	3.60	4.01
10d	91	Insoluble	200	412/402	$C_{40}H_{20}N_2O_8$ (656.61)	Calcd.	73.17	3.07	4.27	—
						Found	72.02	4.38	4.22	—

[a]Measured at c = 20°C with c = 2 g/L in CH_2Cl_2/trifluoroacetic acid (volume ratio 4:1).
[b]Glass-transition temperature from DSC measurements at a heating rate of 20°C/min.
[c]Melting temperature from DSC measurements at a heating rate of 20°C/min.

KRICHELDORF, LINZER, AND BRUHN

TABLE 4. Yields and Properties of Poly(Ester-imide)s 11a–e Prepared from BTCA, 4-Aminophenol, and Various Dicarboxylic Acids

Polymer formula	Yields, %	T_g,[a] °C	T_m,[a] °C	T_i,[b] °C	Elementary formula (formula weight)	Elemental analyses			
							C	H	N
11a	84	200	367(1.H) 358(2.H)	390–400 (dec.)	$C_{42}H_{22}N_2O_9$ (698.65)	Calcd.	72.21	3.17	4.01
						Found	70.73	3.31	4.13
11b	74	221	(332)377	>480 (dec.)	$C_{42}H_{22}N_2O_8S$ (714.71)	Calcd.	70.58	3.10	3.92
						Found	70.01	2.90	3.99
11c	85	–	375	>470 (dec.)	$C_{42}H_{21}ClN_2O_8S$ (749.16)	Calcd.	67.34	2.83	3.74
						Found	66.88	2.75	3.28
11d	72	202	368	395–405 (dec.)	$C_{48}H_{26}N_2O_9$ (774.74)	Calcd.	74.42	3.38	3.62
						Found	73.35	3.86	3.83
11e	81	–	>500 (341)[c]	–	$C_{40}H_{20}N_2O_8$ (656.61)	Calcd.	73.17	3.07	4.27
						Found	71.89	3.41	4.23

[a]From DSC measurements with a heating rate of 20°C/min (1 H = first heating).
[b]From Optical microscopy with crossed polarizers at a heating rate of 10 or 20°C/min (dec. = decomposition).
[c]The first heating curve displays an endotherm which is not reproducible in the second heating trace after cooling at 20°C/min.
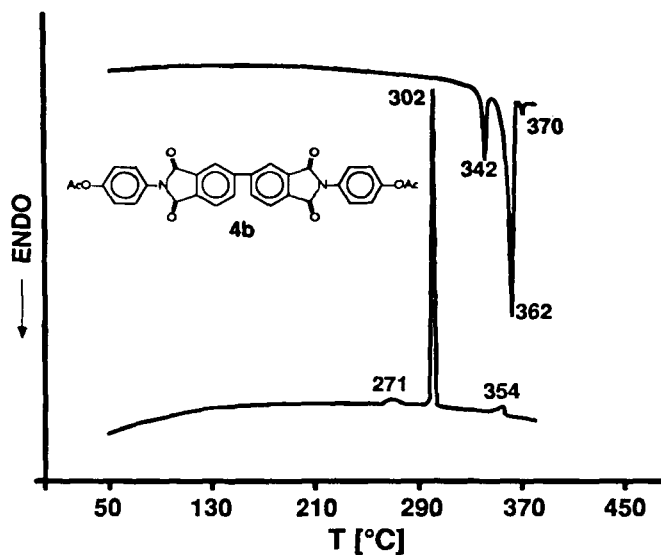
FIG. 1. DSC curves of monomer **4b** measured with a heating and cooling rate of 20°C/min.
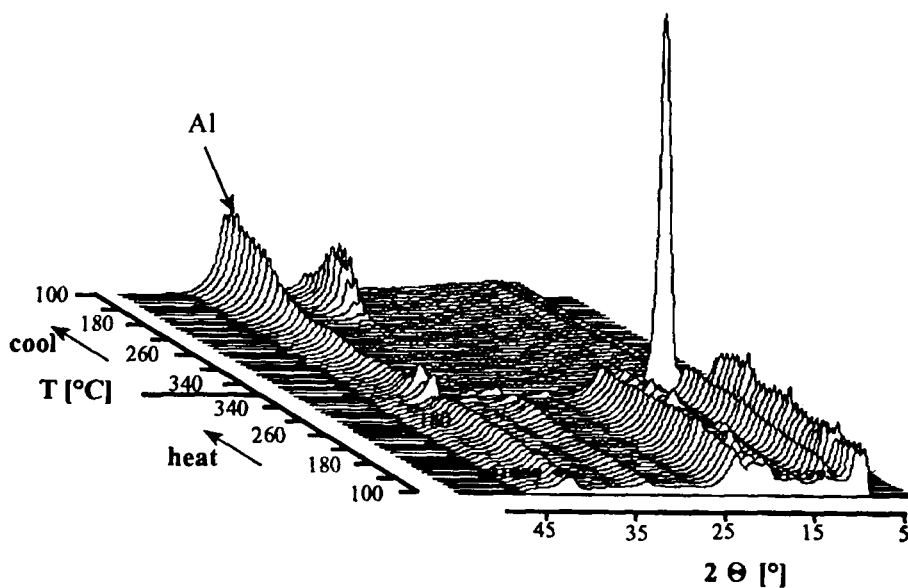

FIG. 2. WAXS powder patterns of monomer **4b** measured with synchrotron radiation ($\lambda = 1.50$ Å) at a heating and cooling rate of 20°C/min (maximum temperature: 378°C).

0.99 / 89.2 Å   3.16 / 28.03 Å

FIG. 3.   SAXS powder patterns monomer **4b** measured with synchrotron radiation (λ = 1.50 Å) at a heating and cooling rate of 20°C/min (maximum temperature: 378°C).
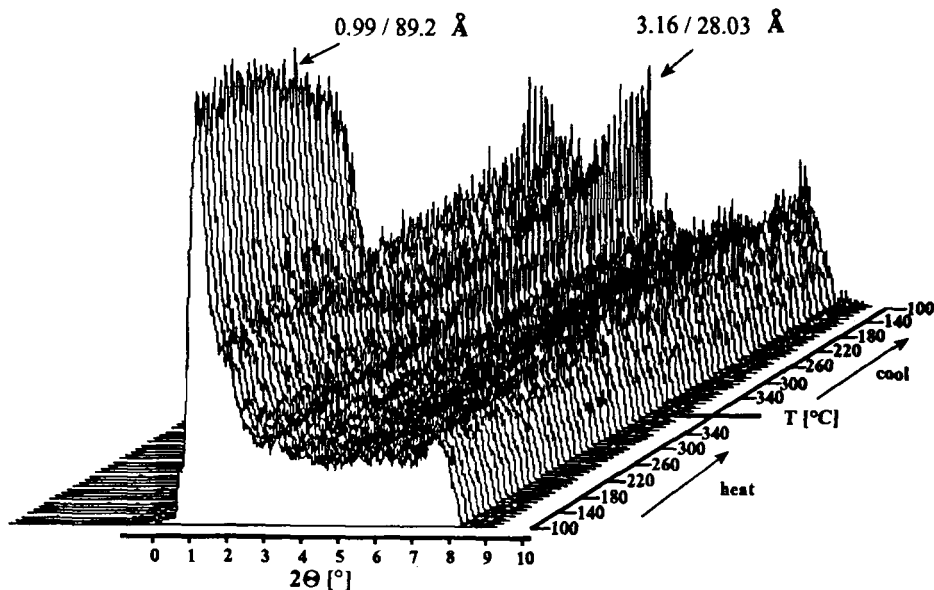
Optical microscopy with crossed polarizers displayed the formation of a new, relatively viscous texture above the melting point at 342°C. This texture may be labeled "batonet texture." It is not a mobile schlieren texture, and thus, agrees with the formation of a smectic phase between 342 and 362°C. At higher temperatures a highly mobile birefringent phase is formed along with an isotropic melt which is the only phase above 375°C. Hence, the phase transition at 370°C in Fig. 1 represents the isotropization process. A clear-cut identification of the anisotropic phase between 362 and 370°C was not feasible because of the biphasic character of the melt and the rapid formation of gas bubbles. The observation of a low viscous melt with schlieren texture and the strong endotherm at 362°C fit in with a transition from a smectic to a nematic phase.

However, it should be emphasized that the entire characterization of **4b** above the melting point is affected by thermal degradation. The SAXS and WAXS patterns obtained upon cooling disagree completely with those of the intact monomer. Furthermore, when the IR spectra of the material recovered from the DSC measurements were measured, they indicated significant changes of the chemical structure. These observations also suggest that at least the initial stage of the polycondensation should be conducted below 300°C.

Properties of Poly(Ester-imide)s

Most poly(ester-imide)s synthesized in this work proved to be insoluble in all common solvents. Therefore, inherent viscosities were only measured in the case of **10a-c**. The moderate values obtained for these three polymers are listed in Table 3 together with elemental analyses and other properties of **9a**, **9b**, and **10a-d**. The

relatively good solubilities of **10a-c** in mixtures of chlorinated alkanes (e.g., CHCl₃) and trifluoroacetic acid fit in with the amorphous character of these poly(ester-imide)s. The amorphous character of **10a-c** was confirmed by WAXS and DSC measurements and agrees with the transparency of these materials.

In contrast to **10a-c**, the poly(ester-imide)s **9a**, **9b**, and **10d** are semicrystalline. The DSC measurements of crude **9a** display a strong melting endotherm at 400°C. The crystallinity vanished after cooling at a rate of 20°C/min and reappeared after annealing above the glass-transition temperature. The WAXS powder pattern of Fig. 4 suggests 20–30% crystallinity. Optical microscopy with crossed polarizers revealed an isotropic melt. In the case of **9b**, no endotherm or exotherm is detectable and no melting process is observable by optical microscopy up to 500°C, but the WAXS powder pattern indicates a certain degree of crystallinity. This is also true for **10d**, and the DSC heating traces exhibit two endotherms (355 and 415°C) in the first and one endotherm (402°C) in the second heating curve (Table 1). Optical microscopy clearly revealed an isotropic melt above 410°C. Thus, all poly(ester-imide)s derived from 3-aminophenol have in common that the melt is isotropic.

All poly(ester-imide)s derived from *p*-aminophenol (**11a-e**) have semicrystallinity in common. The WAXS powder patterns suggest a degree of crystallinity on the order of 20–40% as illustrated in Fig. 5 for poly(ester-imide) **11b**. The first heating traces of the DSC measurements display at least one endotherm between 300 and 400°C (Figs. 6 and 7) in addition to a glass transition step in all cases. Optical microscopy revealed that this endotherm indicates a melting process. In the case of **11b** the melting occurs at the temperature of the strong endotherm around 377°C (Fig. 5), whereas the optical observation did not provide any information on the meaning of the weak endotherm (333°C) and of the weak exotherm (312°C). WAXS measurements conducted with synchrotron radiation at a heating and cool-
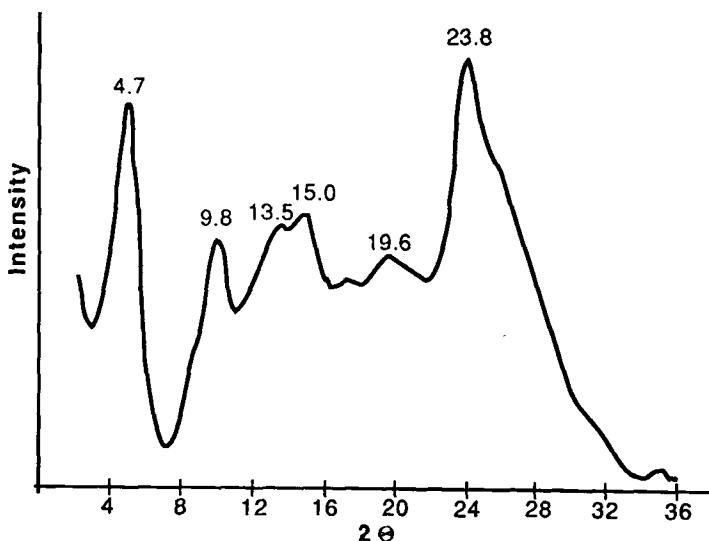

FIG. 4. WAXS powder patterns (measured at 20°C with CuK_α radiation) of poly-(ester-imide) **9a**.
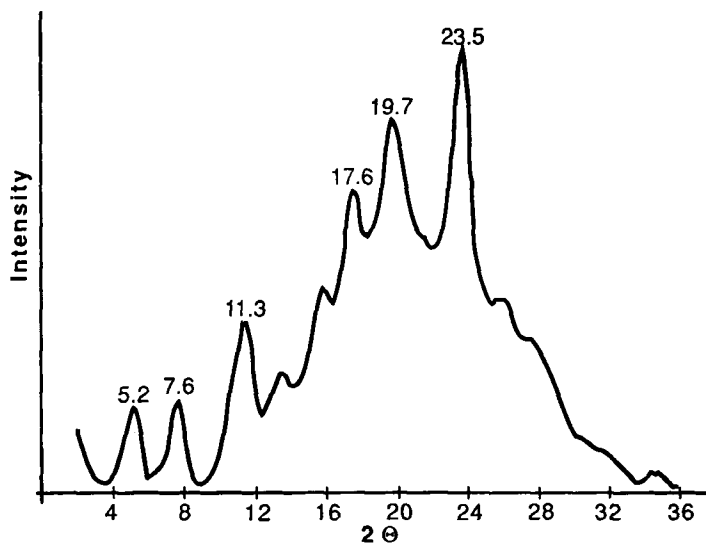
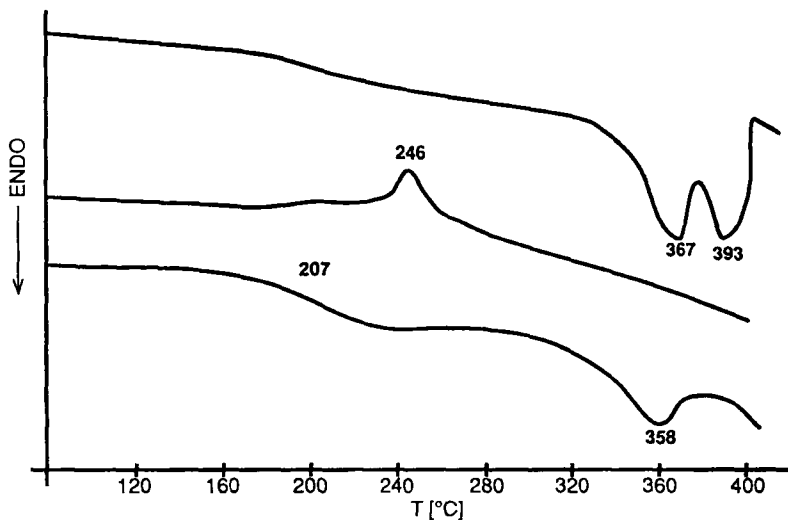FIG. 5.   WAXS powder pattern of poly(ester-imide) **11b** measured at 20°C with CuK$_\alpha$ radiation.

FIG. 6.   DSC curves of poly(ester-imide) **11a** measured at a heating (cooling) rate of 20°C/min: (top) first heating, (middle) first cooling, (bottom) second heating.
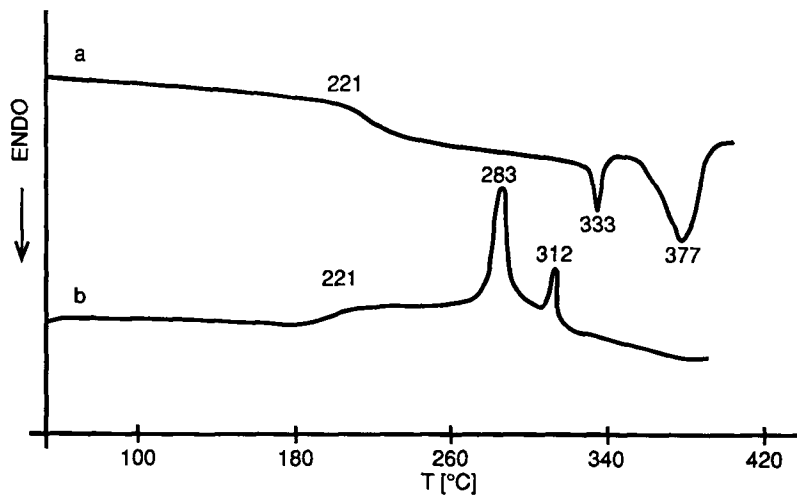
FIG. 7.   DSC curves of poly(ester-imide) **11b** measured at a heating (cooling) rate of 20°C/min: (a) first heating, (b) first cooling.
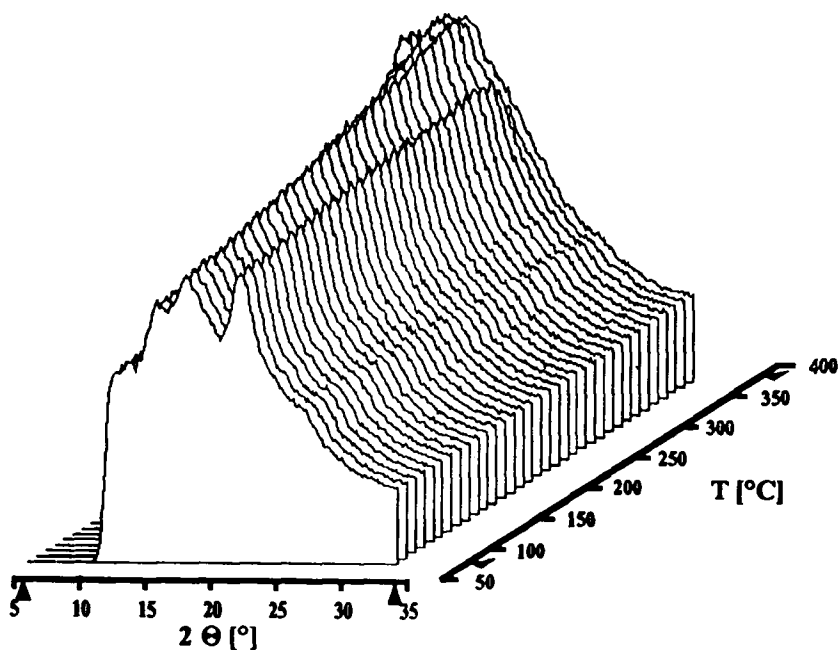

FIG. 8.   WAXS powder patterns of poly(ester-imide) **11b** measured with synchrotron radiation (λ = 1.50 Å) at a heating rate of 20°C/min up to 380°C.

ing rate of 20°C/min confirm this interpretation (Fig. 8). All reflection disappear in the 360–380°C range, in agreement with the formation of a nematic melt. Crystallization occurs around 280°C. Even the WAXS patterns do not say anything about the endotherm at 333°C or the exotherm at 312°C. SAXS patterns measured with synchrotron radiation confirm that the middle-angle reflections typical for smectic layer structures are absent in the solid state and in the melt.

The first heating trace of **11a** displays a second endotherm around 400°C. In this case, optical microscopy revealed that the second endotherm represents the isotropization of a nematic phase whereas the first endotherm represents the melting process. In the case of **11a**, **11c**, and **11d**, only one endotherm is clearly detectable in the DSC curves, which according to optical microscopy indicates the melting process (T_m). The isotropic is not clearly evidenced in the DSC traces because of thermal degradation. Optical microscopy confirmed for **11a**, **11c**, and **11d** the formation of a threadlike schlieren texture above T_m, in analogy to **11b**.

A melting process for **11e** was not detectable up to 500°C. Yet even in the cases of **11a–d**, the melting points are so high that any processing from the melt will be affected by thermal degradation. A further modification of the chemical structure with the purpose of lowering the melting points but maintaining a nematic phase will be discussed in the next paper of this series.

REFERENCES

[1] R. S. Irwin, U.S. Patent 4.178.223 (1979), to DuPont de Nemours Co.
[2] W. Makoto, K. Fujiwara, and H. Hideo, European Patent 314,173 (1989), to Idemitsu Petrochemical Corp.
[3] H. R. Kricheldorf and R. Hüner, *Makromol. Chem., Rapid Commun., 11*, 211 (1990).
[4] H. R. Kricheldorf, A. Domschke, and G. Schwarz, *Macromolecules, 24*, 1011 (1991).
[5] J. de Abajo, J. de la Campa, H. R. Kricheldorf, and G. Schwarz, *Eur. Polym. J., 28*, 261 (1992).
[6] H. R. Kricheldorf and R. Hüner, *J.Polym. Sci., Polym. Chem. Ed., 30*, 337 (1992).
[7] H. R. Kricheldorf, G. Schwarz, and F. Ruhser, *Ibid., 26*, 1621 (1988).
[8] H. R. Kricheldorf and D. Lübbers, *Makromol. Chem., Rapid Commun., 12*, 691 (1991).
[9] H. R. Kricheldorf, F. Ruhser, G. Schwarz, and T. Adebahr, *Makromol. Chem., 192*, 2371 (1991).